

Iteratively Decoded Irregular Variable Length Coding and Trellis Coded Modulation

R. G. Maunder, J. Wang, S. X. Ng, L-L. Yang and L. Hanzo

School of ECS, University of Southampton, SO17 1BJ, UK.

Tel: +44-23-8059 3125, Fax: +44-23-8059 4508

Email: {rm02r,jw02r,sxn,lly,lh}@ecs.soton.ac.uk, <http://www-mobile.ecs.soton.ac.uk>

Abstract – In this paper we propose a novel Irregular Variable Length Coding (IrVLC) scheme for near-capacity joint source and channel coding. We employ a number of Variable Length Coding (VLC) component codebooks having different coding rates for encoding appropriately chosen fractions of the input source symbols. These fractions may be designed With the aid of EXtrinsic Information Transfer (EXIT) charts so that the EXIT curve shape of the IrVLC codec may be matched to that of a serially concatenated channel codec as closely as possible. In this way, an open EXIT chart tunnel may be created even at low E_b/N_0 values that are close to the channel capacity. We detail the proposed serially concatenated and iteratively decoded IrVLC and Trellis Coded Modulation (TCM) designs that are capable of operating within 0.6 dB of the uncorrelated narrowband Rayleigh fading channel's capacity at an effective bandwidth efficiency of 1.56 bit/s/Hz, assuming ideal Nyquist filtering. By contrast, the equivalent-rate VLC-based bench-marker schemes were found to be capable of operating at 1.1 dB from capacity, which is nearly double the discrepancy of the proposed IrVLC-TCM scheme.

1. INTRODUCTION

Irregular Convolutional Coding (IrCC) [1] has been proposed for employment in iteratively decoded joint channel coding and pre-coded equalisation [2]. The IrCC scheme amalgamates a number of component Convolutional Codes (CC) having different coding rates, each of which encodes an appropriately selected fraction of the input bit stream. More specifically, the appropriate fractions may be selected with the aid of EXtrinsic Information Transfer (EXIT) chart analysis [3], by ensuring that the EXIT curve of the composite IrCC may be accurately matched to that of a pre-coded equaliser. In this way, an open EXIT chart tunnel [4] may be created at low E_b/N_0 values using iterative-decoding. As a result, a low Bit Error Ratio (BER) may be achieved at E_b/N_0 values within 1 dB of the Inter Symbol Interference (ISI) contaminated Additive White Gaussian Noise (AWGN) channel's capacity [5].

The financial support of the EPSRC, Swindon UK and the EU under the auspices of the PHOENIX and NEWCOM projects is gratefully acknowledged.

In this contribution we apply the irregular coding concept to joint source and channel coding. We employ a novel Irregular Variable Length Coding (IrVLC) scheme, which is serially concatenated [6] [7] with a bandwidth-efficient Trellis Coded Modulation (TCM) [8] scheme for the sake of exchanging extrinsic information.

In conventional Variable Length Coding (VLC), the source symbols are represented by binary codewords of varying lengths. Short VLC codewords are assigned to frequently occurring source symbol values, whilst long codewords are mapped to infrequently occurring values. In this way the average VLC codeword length L approaches the source entropy E . However, any unintentional residual or intentionally introduced redundancy results in a discrepancy between L and E , which may be exploited to provide an additional error correcting capability during decoding [9]. This error correcting capability is related to and hence may be quantified by the VLC coding rate of $R = E/L \in [0, 1]$, with lower rates corresponding to a higher error correcting capability.

In analogy to joint channel coding and pre-coded equalisation [2], the proposed IrVLC scheme employs a number of VLC codebooks having different coding rates, which are used for encoding appropriately selected fractions of the input source symbols. In this way, the resultant composite EXIT curve may be shaped for the sake of matching that of the channel codec. As in joint channel coding and pre-coded equalisation, this approach allows the amalgamated scheme to operate close to the channel capacity.

The rest of this paper is outlined as follows. In Section 2, we introduce the proposed serially concatenated and iteratively decoded IrVLC-TCM scheme and the appropriate regular VLC-TCM bench-mark scheme. The design and EXIT chart aided characterisation of these schemes is detailed in Section 3. In Section 4, we quantify the attainable performance improvements offered by the proposed IrVLC-TCM arrangements compared to the VLC-TCM bench-marker schemes. Finally, we offer our conclusions in Section 5.

2. SYSTEM OVERVIEW

In this section we provide an overview of a number of serially concatenated and iteratively decoded joint source and channel coding schemes. In each scheme, the inner channel codec

is constituted by TCM [8], which accommodates redundancy by increasing the number of modulation levels, instead of increasing the bandwidth required. The schemes considered differ in their choice of the outer source codec. Specifically, we consider a novel IrVLC codec and an equivalent regular VLC-based bench-marker in this role. In both cases we employ both Symbol-Based (SB) and Bit-Based (BB) VLC decoding, resulting in a total of four different configurations. We refer to these four schemes as the SBirVLC-, BBirVLC-, SBVLC- and BBVLC-TCM arrangements, as appropriate. A schematic that is common to each of these four considered schemes is provided in Figure 1.

The schemes considered are designed for facilitating the near-capacity detection of source samples received over an uncorrelated narrowband Rayleigh fading channel. We consider the case of independent identically distributed (i.i.d.) source samples, which may represent the prediction residual error that remains following the predictive coding of audio, speech [10], image or video [11] information, for example. A Gaussian source sample distribution is assumed, since this has widespread applications owing to the wide applicability of the central limit theorem. Note however that with the aid of suitable adaptation, the techniques proposed in this treatise may be just as readily applied to arbitrary source sample distributions.

In the transmitter of Figure 1, the real-valued source samples are quantized to K number of quantization levels in the block Q . The resultant frame of quantized source samples is synonymously referred to as the frame of source symbols \mathbf{s} here. Each source symbol in this frame indexes the particular quantization level \tilde{e}^k , $k \in [1 \dots K]$, that represents the corresponding source sample in the frame \mathbf{e} with the minimum squared error. Owing to the lossy nature of quantization, distortion is imposed upon the reconstructed source sample frame $\tilde{\mathbf{e}}$ that is obtained by the receiver of Figure 1, following inverse quantization in the block Q^{-1} . The total distortion expected depends on both the original source sample distribution as well as on the number of quantization levels K . This distortion may be minimised by employing Lloyd quantization [12]. Here, a $K = 16$ -level Lloyd quantization scheme is employed, which achieves an expected Signal to Quantization Noise Ratio (SQNR) of about 20 dB for a Gaussian source [12]. Note however that with suitable adaptation, the techniques advocated in this treatise may be just as readily applied to arbitrary quantisers. Also note that Lloyd quantization results in a large variation in the occurrence probabilities of the resultant source symbol values. In the case of our $K = 16$ -level quantizer, the source symbol values' occurrence probabilities range from 0.0082 to 0.1019.

In the transmitter of the proposed scheme, the Lloyd-quantized source symbol frame \mathbf{s} is decomposed into $M = 150$ sub-frames $\{\mathbf{s}^m\}_{m=1}^M$, as shown in Figure 1. This decomposition is necessary for the sake of limiting the receiver complexity, since this employs an exponentially increasing number of trellis states as the number of sub-frames reduces [13]. Each

source symbol sub-frame \mathbf{s}^m comprises $J = 100$ source symbols. Hence, the total number of source symbols in a source symbol frame becomes $M \cdot J = 15,000$. As described above, each Lloyd-quantized source symbol in the sub-frame \mathbf{s}^m has a K -ary value $s_j^m \in [1 \dots K]$, where we have $j \in [1 \dots J]$.

The large differences in the source symbol values' occurrence probabilities provided by Lloyd quantization motivate the employment of VLCs. As described in Section 1, we employ N number of VLC codebooks, where we opted for $N = 15$ for the SBirVLC and BBirVLC schemes and $N = 1$ for the regular SBVLC and BBVLC schemes.

Each Lloyd-quantized source symbol subframe \mathbf{s}^m is VLC-encoded using a single VLC codebook \mathbf{VLC}^n , where we have $n \in [1 \dots N]$. In the case of the SBirVLC and BBirVLC schemes, the particular fraction C^n of the set of source symbol sub-frames that is encoded by the specific VLC codebook \mathbf{VLC}^n is fixed and will be derived in Section 3. The specific Lloyd-quantized source symbols having the value of $k \in [1 \dots K]$ and encoded by the specific VLC codebook \mathbf{VLC}^n are represented by the codeword $\mathbf{VLC}^{n,k}$, which has a length of $I^{n,k}$ bits. The $J = 100$ VLC codewords that represent the $J = 100$ Lloyd-quantized source symbols in each source symbol sub-frame \mathbf{s}^m are concatenated to provide the transmission sub-frame $\mathbf{u}^m = \{\mathbf{VLC}^{n,s_j^m}\}_{j=1}^J$.

Owing to the variable lengths of the VLC codewords, each of the $M = 150$ transmission sub-frames typically comprises a different number of bits. In order to facilitate the VLC decoding of each transmission sub-frame \mathbf{u}^m , it is necessary to explicitly convey its length $I^m = \sum_{j=1}^J I^{n,s_j^m}$ to the receiver. Furthermore, this highly error sensitive side information must be reliably protected against transmission errors. This may be achieved using a low rate block code, for example. For the sake of avoiding obfuscation, this is not shown in Figure 1. Note that the choice of the specific number of sub-frames M in each frame constitutes a trade-off between the computational complexity of VLC decoding and the amount of side information that must be conveyed.

In the scheme's transmitter, the $M = 150$ number of transmission sub-frames $\{\mathbf{u}^m\}_{m=1}^M$ are concatenated. As shown in Figure 1, the resultant transmission frame \mathbf{u} has a length of $\sum_{m=1}^M I^m$ bits.

In the proposed scheme, the VLC codec is protected by a serially concatenated TCM codec. Following VLC encoding, the bits of the transmission frame \mathbf{u} are interleaved in the block π of Figure 1 and TCM encoded in order to obtain the channel's input symbols \mathbf{x} , as shown in Figure 1. These are transmitted over an uncorrelated narrowband Rayleigh fading channel and are received as the channel's output symbols \mathbf{y} , as seen in Figure 1.

In the receiver, Soft-In Soft-Out (SISO) TCM- and VLC-decoding are performed iteratively, as shown in Figure 1. Both of these decoders invoke the Bahl-Cocke-Jelinek-Raviv (BCJR) algorithm [14] on the basis of their trellises. Symbol-level trellises are employed in the case of TCM [8], SBirVLC and SB-

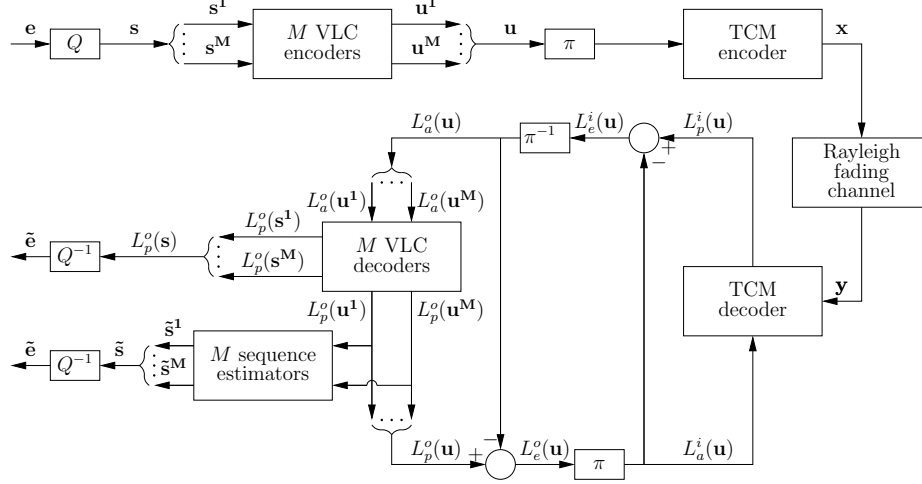


Figure 1: Schematic of the SBIRVLC-, BBIRVLC-, SBVLC- and BBVLC-TCM schemes.

VLC [13] [15] decoding, whilst BBIRVLC and BBVLC decoding rely on bit-level trellises [16]. All BCJR calculations are performed in the logarithmic probability domain and using an eight-entry lookup table for correcting the Jacobian approximation in the Log-MAP algorithm [17].

Soft information, represented in the form of Logarithmic Likelihood Ratios (LLRs) [18], is iteratively exchanged between the TCM and VLC decoding stages for the sake of assisting each other's operation. Upon each successive decoding iteration, the reliability of this soft information increases, until iterative decoding convergence is achieved. In Figure 1, $L(\cdot)$ denotes the LLRs of the bits concerned (or the L-values of the specific symbols as appropriate), where the superscript i indicates inner TCM decoding, while o corresponds to outer VLC decoding. Additionally, a subscript denotes the dedicated role of the LLRs (or L-values), with a , p and e indicating *a priori*, *a posteriori* and extrinsic information, respectively.

During each decoding iteration, the inner TCM decoder is provided with *a priori* LLRs pertaining to the transmission frame $L_a^i(\mathbf{u})$, as shown in Figure 1. These LLRs are obtained from the most recent operation of the outer VLC decoding stage, as will be highlighted below. In the case of the first decoding iteration, no previous VLC decoding has been performed and hence the *a priori* LLRs $L_a^i(\mathbf{u})$ provided for TCM decoding are all zero-valued, corresponding to a probability of 0.5 for both '0' and '1'. Given the channel's output symbols \mathbf{y} and the *a priori* LLRs $L_a^i(\mathbf{u})$, the BCJR algorithm is employed for obtaining the *a posteriori* LLRs $L_p^i(\mathbf{u})$, as shown in Figure 1.

During iterative decoding, it is necessary to prevent the reuse of already exploited information, since this would limit the attainable iteration gain [17]. This is achieved following TCM decoding by the subtraction of $L_a^i(\mathbf{u})$ from $L_p^i(\mathbf{u})$, as shown in Figure 1. The resultant extrinsic LLRs $L_e^i(\mathbf{u})$ are deinterleaved in the block π^{-1} and forwarded as *a priori* LLRs

for VLC decoding.

As stated above, $M = 150$ separate VLC decoding processes are employed in the proposed scheme's receiver. Similarly to the decomposition of the bit-based transmission frame \mathbf{u} into sub-frames, the *a priori* LLRs $L_a^o(\mathbf{u})$ are decomposed into $M = 150$ sub-frames, as shown in Figure 1. This is achieved with the aid of the explicit side information that conveys the number of bits I^m in each transmission sub-frame \mathbf{u}^m . Each of the $M = 150$ VLC decoding processes is provided with the *a priori* LLR sub-frame $L_a^o(\mathbf{u}^m)$ and in response it generates the *a posteriori* LLR sub-frame $L_p^o(\mathbf{u}^m)$, $m \in [1 \dots M]$. These *a posteriori* LLR sub-frames are concatenated in order to provide the *a posteriori* LLR frame $L_p^o(\mathbf{u})$, as shown in Figure 1. Following the subtraction of the *a priori* LLRs $L_a^o(\mathbf{u})$, the resultant extrinsic LLRs $L_e^o(\mathbf{u})$ are interleaved and forwarded as *a priori* information to the next TCM decoding iteration.

In the case of SBIRVLC and SBVLC decoding, each of the $M = 150$ VLC decoding processes additionally provides *a posteriori* L-values pertaining to the corresponding source symbol sub-frame $L_p^o(\mathbf{s}^m)$. This comprises a set of K number of L-values for each source symbol s_j^m in the sub-frame \mathbf{s}^m , where $j \in [1 \dots J]$. Each of these L-values provides the logarithmic probability that the corresponding source symbol s_j^m has the particular value $k \in [1 \dots K]$. In the receiver of Figure 1, the source symbols' L-value sub-frames are concatenated to provide the source symbol L-value frame $L_p^o(\mathbf{s})$. By inverse-quantising this soft information in the block Q^{-1} , a Minimum Mean Squared Error (MMSE) source sample frame estimate $\tilde{\mathbf{e}}$ can be obtained. More specifically, each reconstructed source sample is obtained by using the corresponding set of K source symbol value probabilities to find the weighted average of the K number of quantization levels $\{\tilde{e}^k\}_{k=1}^K$.

Conversely, in the case of BBIRVLC and BBVLC decoding, no symbol-level *a posteriori* output is available. In this

case, the source symbol subframe \mathbf{s}^m must be estimated from the *a posteriori* bit-level output $L_p^o(\mathbf{u}^m)$. This may be achieved by employing symbol-level sequence estimation, as shown in Figure 1. This exploits the explicit knowledge that the subframe \mathbf{s}^m comprises $J = 100$ source symbols, in order to obtain a hard decision estimate $\tilde{\mathbf{s}}^m$. Following concatenation, the source symbol frame estimate $\tilde{\mathbf{s}}$ may be inverse-quantised, in order to obtain the source sample frame estimate $\tilde{\mathbf{e}}$. Note that since this approach relies on hard source symbol decisions prior to inverse-quantization, a higher level of source distortion may be expected than that attained, when employing the soft decisions of the SBiVLC and SBVLC decoders. However, this reduced performance benefits us in terms of a reduced complexity, because a high number of transitions would have to be considered by the symbol-level VLC decoding trellis for generating the related soft-decisions.

In the next section we detail the design of our IrVLC scheme and characterise each of the SBiVLC-, BBiVLC-, SBVLC- and BBVLC-TCM schemes with the aid of EXIT chart analysis.

3. SYSTEM PARAMETER DESIGN

As described in Section 1, the SBiVLC and BBiVLC schemes may be constructed by employing a number of VLC codebooks having different coding rates, each of which encodes an appropriately chosen fraction of the input source symbols. We opted for using $N = 15$ VLC codebooks \mathbf{VLC}^n , $n \in [1 \dots N]$, that were specifically designed for encoding $K = 16$ -level Lloyd-quantized Gaussian i.i.d. source samples. More specifically, the $N = 15$ VLC codebooks comprised 13 Variable Length Error Correcting (VLEC) designs having various minimum block-, convergence- and divergence-distances [19], complemented by a symmetric- and an asymmetric-Reversible Variable Length Coding (RVLC) design [19]. In all codebooks, a minimum free distance of least $d_f = 2$ was employed, since this supports convergence to an infinitesimally low BER [20]. The resultant average VLC codeword lengths of $L^n = \sum_{k=1}^K P(k) \cdot I^{n,k}$, $n \in [1 \dots N]$, were found to range from 3.94 to 12.18 bits. When compared to the source symbol entropy of $E = -\sum_{k=1}^K P(k) \cdot \log_2(P(k)) = 3.77$, these correspond to coding rates of $R^n = E/L^n$ spanning the range of 0.31 to 0.96.

As will be detailed below, our SBiVLC and BBiVLC schemes were designed under the constraint that they have an overall coding rate of $R = 0.52$. This value was chosen, since it is the coding rate of the VLC codebook \mathbf{VLC}^{10} , which we employ in our SBVLC and BBVLC bench-markers using $N = 1$ codebook. This coding rate results in an average interleaver length of $M \cdot J \cdot E/R = 108,750$ bits for all the schemes considered.

In-phase Quadrature-phase (IQ)-interleaved TCM having eight trellis-states per symbol along with 3/4-rate coded 16-Level Quadrature Amplitude Modulation (16QAM) is employed, since this is appropriate for transmission over uncorrelated

narrowband Rayleigh fading channels. Ignoring the modest bitrate contribution of conveying the side information, the bandwidth efficiency of the schemes considered is therefore $\eta = 0.52 \cdot 0.75 \cdot \log_2(16) = 1.56$ bit/s/Hz, assuming ideal Nyquist filtering having a zero excess bandwidth. This value corresponds to the channel capacity of the uncorrelated narrowband Rayleigh fading channel at an E_b/N_0 value of 2.6 dB [21]. Given this point on the corresponding channel capacity curve, we will be able to quantify, how closely the proposed schemes may approach this ultimate limit.

In Figure 2, we provide the EXIT curves $I_e^i(I_a^i, E_b/N_0)$ of the TCM scheme for a number of E_b/N_0 values above the channel capacity bound of 2.6 dB. The inverted EXIT curves $I_a^{o,n}(I_e^o)$ plotted for the $N = 15$ VLC codebooks, together with their coding rates R^n , are also given in Figure 2. Note that these curves were obtained using bit-based VLC decoding, but similar curves may be obtained for symbol-based decoding.

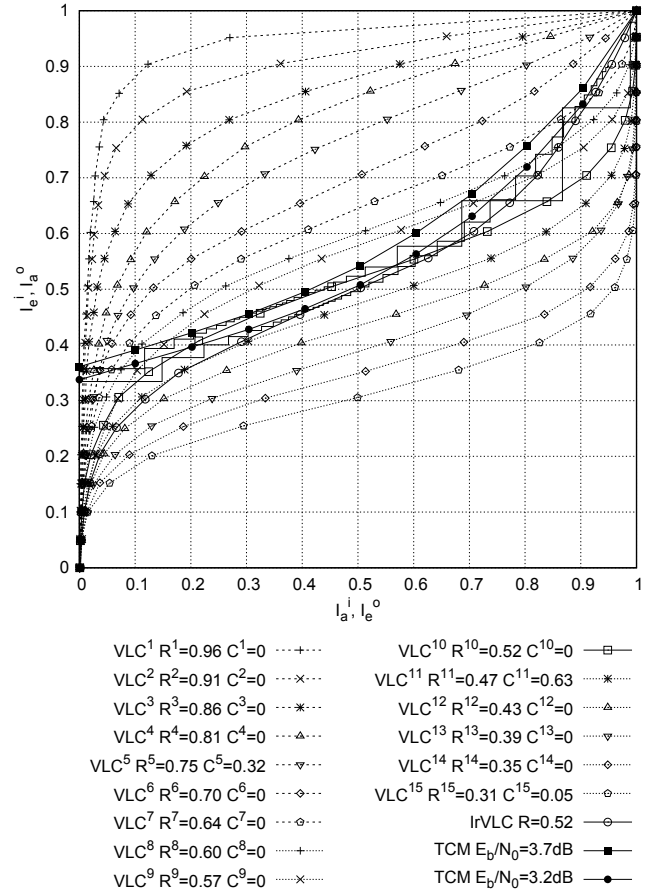


Figure 2: Inverted VLC EXIT curves and TCM EXIT curves.

The inverted EXIT curve of an IrVLC scheme $I_a^o(I_e^o)$ can be obtained as the appropriately weighted superposition of the

$N = 15$ component VLC codebooks' EXIT curves,

$$I_a^o(I_e^o) = \sum_{n=1}^N \alpha^n I_a^{o,n}(I_e^o), \quad (1)$$

where α^n is the fraction of the transmission frame \mathbf{u} that is generated by the specific component codebook \mathbf{VLC}^n . Note that the values of α^n are subject to the constraints

$$\sum_{n=1}^N \alpha^n = 1, \quad \alpha^n \geq 0 \forall n \in [1 \dots N]. \quad (2)$$

The specific fraction of source symbol subframes \mathbf{s}^m that should be encoded by the specific component codebook \mathbf{VLC}^n in order that it generates a fraction α^n of the transmission frame \mathbf{u} , is given by

$$C^n = \alpha^n \cdot R^n / R, \quad (3)$$

where $R = 0.52$ is the desired overall coding rate. Again, the specific values of C^n are subject to the constraints

$$\sum_{n=1}^N C^n = \sum_{n=1}^N \alpha^n \cdot R^n / R = 1, \quad C^n \geq 0 \forall n \in [1 \dots N]. \quad (4)$$

Beneficial values of C^n may be chosen by ensuring that there is an open EXIT tunnel between the inverted IrVLC EXIT curve and the EXIT curve of TCM at an E_b/N_0 value that is close to the channel capacity bound. This may be achieved using the iterative EXIT-chart matching process of [1] to adjust the values of $\{C^n\}_{n=1}^N$ under the constraints of (2) and (4) for the sake of minimising the error function

$$\int_0^1 e(I)^2 dI, \quad (5)$$

where

$$e(I) = I_e^i(I, E_b/N_0) - I_a^o(I) \quad (6)$$

is the difference between the inverted IrVLC EXIT curve and the EXIT curve of TCM at a particular target E_b/N_0 value. Note that in order to ensure that the design results in an open EXIT tunnel, we must impose the additional constraint of

$$e(I) > 0 \forall I \in [0, 1]. \quad (7)$$

Open EXIT tunnels were found to be achievable for both the SBIrVLC- and the BBIrVLC-TCM schemes at an E_b/N_0 of 3.2 dB, which is just 0.6 dB from the channel capacity bound of 2.6 dB. The corresponding values of C^n are provided in Figure 2 and we note that all but three of these are zero-valued. This implies that a low-complexity three-component IrVLC design is capable of approaching the channel's capacity.

By contrast, the corresponding EXIT-tunnel only becomes open for the SBVLC- and BBVLC-TCM bench-markers for E_b/N_0 values in excess of 3.7 dB, which is 1.1 dB from the channel capacity bound of 2.6 dB. We can therefore expect our SBIrVLC- and BBIrVLC-TCM schemes to be capable of operating at nearly half the distance from the channel capacity in comparison to our bench-markers, achieving a gain of about 0.5 dB.

4. RESULTS

The transmission of a single frame of $M \cdot J = 15,000$ source samples \mathbf{e} was simulated over a range of E_b/N_0 values, when communicating over an uncorrelated narrowband Rayleigh fading channel. For each value of E_b/N_0 we consider the reconstructed source sample frame $\tilde{\mathbf{e}}$ and evaluate the Signal to Noise Ratio (SNR) associated with the ratio of the source signal's energy and the reconstruction error that may be achieved following iterative decoding convergence. This relationship is plotted for each of the SBIrVLC-, BBIrVLC-, SBVLC- and BBVLC-TCM schemes in Figure 3.

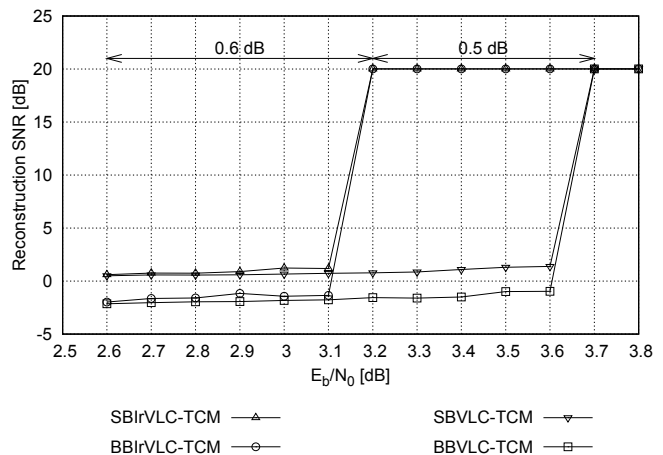


Figure 3: Reconstruction SNR versus E_b/N_0 for a Gaussian source using a $K = 16$ -level Lloyd quantization for the SBIrVLC-, BBIrVLC-, SBVLC- and BBVLC-TCM schemes communicating over an uncorrelated narrowband Rayleigh fading channel.

At sufficiently high E_b/N_0 values, all considered schemes are capable of obtaining an error-free reconstructed source sample frame $\tilde{\mathbf{e}}$ containing only quantization noise, corresponding to an SNR of 20 dB. In the case of the SBIrVLC- and BBIrVLC-TCM schemes, this is achieved for E_b/N_0 values above 3.2 dB, which is just 0.6 dB from the channel capacity bound of 2.6 dB. Again, this represents a 0.5 dB gain in comparison to the performance of the SBVLC- and BBVLC-TCM bench-markers, which achieve an error-free reconstruction for E_b/N_0 values in excess of 3.7 dB.

Note that these findings confirm the EXIT chart predictions of Section 3. Recall that Figure 2 provides decoding trajectories for the BBIrVLC-TCM and BBVLC-TCM schemes at E_b/N_0 values of 3.2 dB and 3.7 dB, respectively. Note that owing to the high interleaver length of $M \cdot J \cdot E/R = 108,750$ bits, the recorded trajectories have a close match with the corresponding TCM and inverted IrVLC/VLC EXIT curves. In both cases, the corresponding trajectory can be seen to converge to the (1,1) mutual information point of the EXIT chart after a number of decoding iterations.

At low E_b/N_0 values, the corresponding TCM EXIT curves cross the inverted IrVLC/VLC EXIT curves and the open EXIT chart tunnel disappears. In these cases, iterative decoding convergence to unity mutual information cannot be achieved, resulting in the poor reconstruction quality that may be observed at low values of E_b/N_0 in Figure 3. It is in this low E_b/N_0 region that the SBIrVLC- and SBVLC-TCM schemes outperform the BBIrVLC- and BBVLC-TCM schemes. The improved performance of the SBIrVLC and SBVLC decoders is a benefit of their ability to provide symbol-level soft-decision outputs instead of hard-decisions. However, this is attained at the cost of a complexity that was found to be an order of magnitude higher than that of the BBIrVLC and BBVLC decoders, when considering the number of Add-Compare-Select (ACS) operations, which is one of the most pertinent complexity metrics in the context of systolic-array-type silicon chips. In the light of this, the employment of the SBIrVLC-TCM scheme instead of the BBIrVLC-TCM scheme appears unattractive.

5. CONCLUSIONS

In this paper we have introduced a novel IrVLC design for near-capacity joint source and channel coding. In analogy to IrCC coding invoked for joint channel coding and pre-coded equalisation [2], IrVLC employs a number of component VLC codebooks having different coding rates in appropriate proportions. More specifically, with the aid of EXIT chart analysis, the appropriate fractions of the input source symbols may be chosen for directly ensuring that the EXIT curve of the IrVLC codec may be matched to that of a serially concatenated channel codec. In this way, an open EXIT chart tunnel facilitating near-capacity high quality source reconstruction may be achieved.

We have detailed the construction of an IrVLC scheme that is suitable for the encoding of 16-level Lloyd quantized Gaussian i.i.d. source samples and for use with IQ-interleaved TCM and 16QAM over uncorrelated narrowband Rayleigh fading channels. For the purposes of comparison, we also selected a regular VLC bench-marker, having a coding rate equal to that of our IrVLC scheme. Serially-concatenated and iteratively decoded SBIrVLC-, BBIrVLC-, SBVLC- and BBVLC-TCM schemes were characterised with the aid of EXIT chart analysis. These schemes have a bandwidth efficiency of 1.56 bits per channel symbol, which corresponds to a Rayleigh fading channel capacity bound of 2.6 dB. The SBIrVLC- and BBIrVLC-TCM schemes were found to offer high-quality source reconstruction at an E_b/N_0 value of 3.2 dB, which is just 0.6 dB from capacity. This compares favourably with the SBVLC- and BBVLC-TCM bench-markers, which require an E_b/N_0 value of 3.7 dB. Owing to the higher computational complexity of the SBIrVLC-TCM scheme, the BBIrVLC-TCM arrangement was identified as our preferred scheme.

6. REFERENCES

- [1] M. Tüchler and J. Hagenauer, "EXIT charts of irregular codes," in *Conference on Information Sciences and Systems*, (Princeton, NJ), pp. 748–753, March 2002.
- [2] J. Wang, S. X. Ng, A. Wolfgang, L.-L. Yang, S. Chen, and L. Hanzo, "Near-capacity three-stage MMSE turbo equalization using irregular convolutional codes," in *International Symposium on Turbo Codes*, (Munich, Germany), April 2006.
- [3] S. ten Brink, "Convergence of iterative decoding," *Electronics Letters*, vol. 35, no. 10, pp. 806–808, 1999.
- [4] A. Ashikhmin, G. Kramer, and S. ten Brink, "Extrinsic information transfer functions: model and erasure channel properties," *IEEE Transactions on Information Theory*, vol. 50, pp. 2657–2673, November 2004.
- [5] C. E. Shannon, "The mathematical theory of communication," *Bell System Technical Journal*, vol. 27, pp. 379–423, July 1948.
- [6] S. Benedetto and G. Montorsi, "Serial concatenation of block and convolutional codes," *Electronics Letters*, vol. 32, no. 10, pp. 887–888, 1996.
- [7] S. Benedetto and G. Montorsi, "Iterative decoding of serially concatenated convolutional codes," *Electronics Letters*, vol. 32, no. 13, pp. 1186–1188, 1996.
- [8] G. Ungerboeck, "Channel coding with multilevel/phase signals," *IEEE Transactions on Information Theory*, vol. 28, no. 1, pp. 55–67, 1982.
- [9] V. Buttigieg and P. G. Farrell, "Variable-length error-correcting codes," *IEE Proceedings on Communications*, vol. 147, pp. 211–215, August 2000.
- [10] L. Hanzo, F. C. A. Somerville, and J. P. Woodard, *Voice Compression and Communications: Principles and Applications for Fixed and Wireless Channels*. IEEE Press-John Wiley & Sons., 2001.
- [11] L. Hanzo, P. J. Cherriman, and J. Streit, *Wireless Video Communications: Second to Third Generation and Beyond*. Piscataway, NJ: IEEE Press-John Wiley & Sons, 2001.
- [12] S. Lloyd, "Least squares quantization in PCM," *IEEE Transactions on Information Theory*, vol. 28, no. 2, pp. 129–137, 1982.
- [13] R. Bauer and J. Hagenauer, "Symbol by symbol MAP decoding of variable length codes," in *3rd ITG Conference on Source and Channel Coding*, (Munich, Germany), pp. 111–116, January 2000.
- [14] L. Bahl, J. Cocke, F. Jelinek, and J. Raviv, "Optimal decoding of linear codes for minimizing symbol error rate (Corresp.)," *IEEE Transactions on Information Theory*, vol. 20, no. 2, pp. 284–287, 1974.
- [15] J. Kliewer and R. Thobaben, "Iterative joint source-channel decoding of variable-length codes using residual source redundancy," *IEEE Transactions on Wireless Communications*, vol. 4, no. 3, pp. 919–929, 2005.
- [16] R. Bauer and J. Hagenauer, "On variable length codes for iterative source/channel decoding," in *Data Compression Conference*, (Snowbird, UT), pp. 273–282, March 2001.
- [17] L. Hanzo, T. H. Liew, and B. L. Yeap, *Turbo Coding, Turbo Equalisation and Space Time Coding for Transmission over Wireless Channels*. Chichester, UK: Wiley, 2002.
- [18] J. Hagenauer, E. Offer, and L. Papke, "Iterative decoding of binary block and convolutional codes," *IEEE Transactions on Information Theory*, vol. 42, no. 2, pp. 429–445, 1996.
- [19] J. Wang, L.-L. Yang, and L. Hanzo, "Iterative construction of reversible variable-length codes and variable-length error-correcting codes," *IEEE Communications Letters*, vol. 8, pp. 671–673, November 2004.
- [20] R. Thobaben and J. Kliewer, "Low-complexity iterative joint source-channel decoding for variable-length encoded Markov sources," *IEEE Transactions on Communications*, vol. 53, pp. 2054–2064, December 2005.
- [21] L. Hanzo, S. X. Ng, T. Keller, and W. Webb, *Quadrature Amplitude Modulation*. Chichester, UK: Wiley, 2004.